SVU-International Journal of Engineering Sciences and Applications (2020) 2(2): 70-75
Print ISSN 2785-9967 | Online ISSN 2735-4571
DOI 10.21608/svusrc.2021.94632.1017

Compact 500 MHz Coupled Resonators Design Analyzed by J-Inverters for Wireless Power Transfer (WPT) Utilization

Mahmoud M. A. El-Negm[1], Hany A. Atallah[1*], Adel B. Abdel-Rahman[1,2]
(0000-0001-5541-2326, 0000-0002-1235-7627)

Abstract In this work, a compact structure employing complementary split ring resonator defected ground structure (CSRR-DGS) and loaded with a chip capacitor for wireless power transfer (WPT) applications is suggested and discussed. The CSRR is loaded with a surface mounted (SMD) capacitor for miniaturization purposes. The proposed design is analyzed by J-inverters for verifications. The values of the extracted J-inverters for the proposed arrangement are calculated based on the mutual coupling among the transmitter (TX) and the receiver (RX). The prototype is fabricated and confirmed for validations. The model is designed at a center frequency of 500 MHz. The complete design has a total size of 25 × 25 m^2. The proposed design achieves a coupling efficiency of about 97 % at a transmission distance of 16 mm. Good agreements among the electromagnetic (EM) simulation and the measurements have been attained. The suggested design is appropriate for short range WPT applications.

Keywords: Coupling efficiency; transmission distance; wireless power transfer (WPT).

1 Introduction

Wireless communication standards have attracted great attention in the previous periods for its significance in essential utilization such as movable electronic equipment, RFID, implantable biomedical requests, and so on [1–10]. The different techniques of the wireless systems can be classified into 1- Inductive and capacitive coupling are helpful for short-range [11], [12]. 2- Resonant coupling is beneficial for mid-range [13]. 3- Light waves and microwaves are applicable for long-range [14], [15]. Many wireless systems have utilized inductors, capacitors, and spirals [6], [16], and [17]. Several of the recently available papers in the field of Wireless electricity have used DGSs. DGSs are the incisions that are merged on the lower surface of the substrate. The setting of DGS shapes below the feed line is presented variation in the prevalence of the waves along the line improving some characteristics in the circuit [18–25], and [4–6]. Inductors and capacitors attached to DGSs are requested for modern RF/Microwave for performing filtering characteristics through small designs [18], [19].

The H-shaped samples are operated at a 1 GHz band with 85% efficiency and 25 mm × 25 mm system size for Wireless systems [22]. Two prototypes are considered for wireless appliances. The H sample has a substrate size of 20 mm× 20 mm and an efficiency of 68 % at distance equal to 1.3 cm. However, the semi H-pattern accomplishes an enhanced efficiency of around 73 % with the board size is 21 × 21 mm^2 at a 25 mm perpendicular distance [26]. The authors in [24] present a unique model that includes two combined C-shaped resonators with an efficient coupling of 69 % at a 1.5 cm vertical distance. Though, the prototype size is 2.5 cm × 2.5 cm to permits the transmission of the power wirelessly. In [27], the authors present a novel structure for wireless electricity that depends on the symmetric model. The size is 120 mm × 120 mm for

Received: 7 September 2021/ Accepted: 5 December 2021
* Corresponding Author: Hany A. Atallah,
h.atallah@eng.svu.edu.eg
1. Electrical Engineering Department, Faculty of Engineering, South Valley University, Qena 83523, Egypt

2. Department of Electronics and Communications, Egypt-Japan University of Science and Technology, Alexandria Egypt

TX, and the size is 80 mm × 80 mm for RX while the system works at a transmission distance of 30 mm and coupling efficiency of 54.5 %. The author in [28] studied a model depending on dual-frequency resonators for biotelemetry requests. In [29], the author introduced a significant application for wireless electricity and the ways for powering sensors that are entrenched in buildings by employing rechargeable batteries.

In this work, the proposed model can be utilized for WPT arrangements by employing the j-inverter technique. Firstly, theoretical proof and the prototype of the resonator are illustrated. The model is simulated by using Computer Simulation Technology (CST), and the separation among the TX unit and RX unit is studied to attain better efficiency. Subsequently, the suggested design has been measured after fabrication. Good agreement among the simulation data and measurement is achieved with suitable concurrence. Finally, the conclusion of the work is summarized.

2 Design and Methods

The microstrip feed line has a dimension of ($Wf \times Lf$) at the top side of the patch that is associated with the fifty-ohm port (P1). The feed line Lf is influential such as element capacitor C_S and operated for matching the impedance by modifying its distance as demonstrated in Fig. 1(a). The CSRR-DGS is excavated on the underside of the design with added a constant capacitor of 9 pF welded in the outer circle to boost equivalent capacitance without increase the basic size of the pattern as an display in Fig. 1(b). The prototype is realized and achieved by using an advanced design system (ADS) as shown in Fig. 1(c). The substrate measurements in Table 1 have applied to result in one pole band-stop filter BSF with 550 MHz.

Table 1 The used values and material

Parameter	Value	Parameter	Value / Type
Lsub	25 mm	*T1*	1 mm
Wsub	25 mm	*T2*	1.5 mm
Wf	1.8 mm	*G*	2 mm
Lf	19 mm	*Substrate*	*FR4*
R1	6.5 mm	*Sub thickness*	0.8 mm
R2	10.8 mm	*Subs εr*	4.3

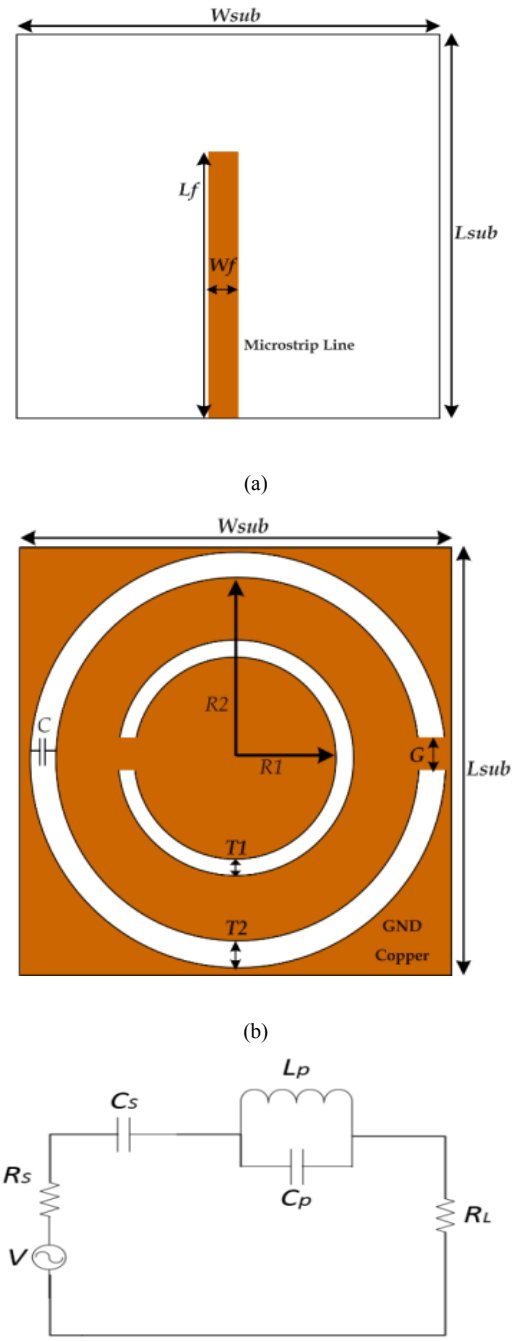

Fig. 1 Layout of the resonator and its equivalent circuit (a) Top side (b) Bottom side (c) Equivalent circuit model ECM.

3 Coupled Resonators Design

As illustrated in Fig. 2, the execution of the presented coupled resonators employing CST and ECM of the model. When a single band stop filter S-BSF is combined back-to-back configuration, it transfers to a BPF leading to a highly efficient and compact size.

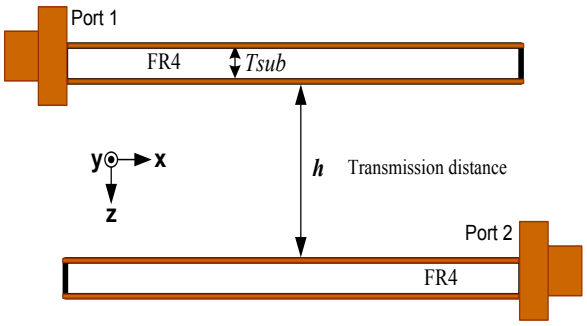

(a)

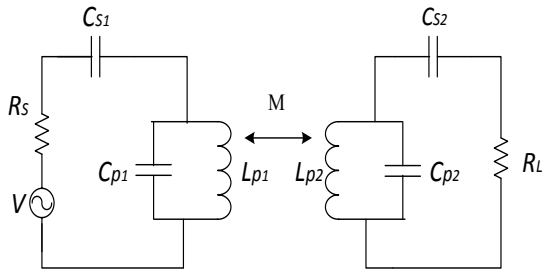

(b)

Fig. 2 Execution of the proposed resonator (a) 3-D view (b) ECM

The coupling is tested by moving the area (h) between RX and TX; it is strong at convergent regions while it is weak in far areas as sketched in Fig. 3.

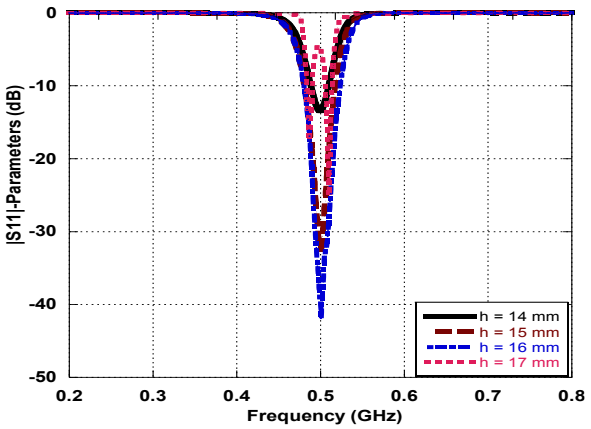

(a)

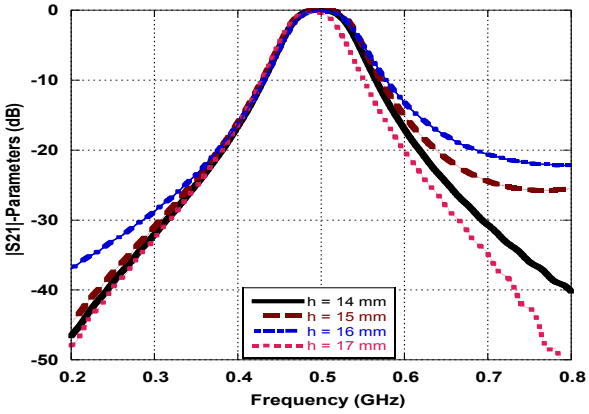

(b)

Fig. 3 Separation study of the coupled resonators (a) $|S_{11}|$ (b) $|S_{21}|$

4 J-inverter ECM

In this partition, the J-inverters technique will be utilized to single-band WPT requests. WPT happens as understand from the equivalent circuit in Figure 4(a) that collected capacitances $C_{P1} = C_{P2}$, inductances $L_{P1} = L_{P2}$, and mutual coupling represented by M. we replace the stub that caused from MSL with the capacitors C_S and is computed by (1). Where f_o is the resonant frequency, and β is the phase shift constant. The MSLs are disconnected, Z-parameters are employed, and the circuit ingredients are isolated as $M = (I_m Z)/(2\pi f)$.

$$C_{s1} = C_{s2} = \frac{\tan \beta l stub}{2\pi f_o Z_o} \quad (1)$$

Fig. 4(b) appears the ECM and the element of the J-inverter occupied at the frequencies ω_o that can be computed by equations (2) and (3) [27]. Figure 4 (c) explains 3 cascaded ingredients of the J-inverters J_{S2}, J_{S1}, and J_m. the output J-inverter is J_{S2}, the input J-inverter is J_{S1} that are united coupling capacitors. J_m Is the intermediary J-inverter that is joined to mutual coupling among the resonators.

At $\omega = \omega_0$

$$L_a = \frac{L_{p1}L_{p2} - M^2}{L_{p2} - M} \qquad L_b = \frac{L_{p1}L_{p2} - M^2}{L_{p1} - M}$$

$$L_m = \frac{L_{p1}L_{p2} - M^2}{M} \quad (2)$$

$$C_{s1} = \frac{J_{s1}}{\omega_0 \sqrt{1 - (J_{s1}R_0)^2}} \qquad C_{s2} = \frac{J_{s2}}{\omega_0 \sqrt{1 - (J_{s2}R_0)^2}}$$

$$C_{sec1} = \frac{C_{s1}}{1 + (\omega_0 C_{s1} R_0)^2} \quad C_{sec2} = \frac{C_{s2}}{1 + (\omega_0 C_{s1} R_0)^2} \qquad (3)$$

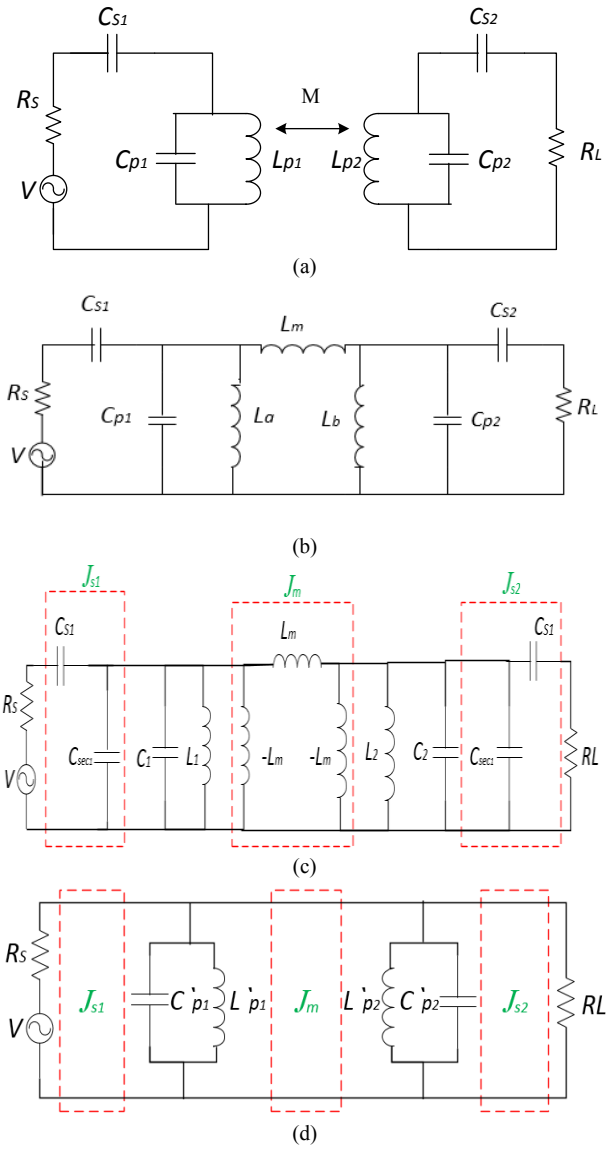

Fig. 4 (a) The equivalent circuit conversion employing J-inverters. (b) The π equivalent circuit of the model. (c) The equivalent circuit employing J-inverters. (d) The reduced equivalent circuit at ω_o.

The scheme in Figure 4(c) can be abridged to Figure 4(d). The parameters in Figure 4(c) are evaluated by equation (4) [27]. Henceforth, at ω_0 the J-inverter (J_m) will be indicated by L_m.

$$C`_{P1} = C_1 + C_{sec1}, \quad C`_{P2} = C_2 + C_{sec2}$$
$$L`_{p1} = L_1 - \frac{M^2}{L_2}, \quad L`_{p2} = L_2 - \frac{M^2}{L_1}$$

$$J_m = \frac{1}{L_m \omega_0} \qquad (4)$$

To emphasize maximum coupling efficiency, the input admittance monitoring from the source in Figure 5(c) equals 1/Rs as in equation (5). The values of J-inverters for the pattern are scheduled in Table 2 where $Z_0 = R_S = R_L = 50\ \Omega$ and in symmetric $J_{S2} = J_{S1} = J_m/R$.

$$Y_{s2} = \frac{{J_{s2}}^2}{1/R} = {J_{s2}}^2 R$$
$$Y_m = \frac{{J_m}^2}{Y_{s2}} = \frac{{J_m}^2}{{J_{s2}}^2 R}$$
$$Y_{s1} = Y_{in} = \frac{{J_{s1}}^2}{Y_m} = \frac{{J_{s1}}^2 {J_{s2}}^2 R_L}{{J_m}^2} = \frac{1}{R_s} \qquad (5)$$

Table 2 J-Inverter values for the suggested structure

J_m	$J_{S1} = J_{S2}$
At 0.5GHz	At 0.5GHz
0.0007	0.0037
Cp1=Cp2 (pF)	*CS1=CS2* (pF)
7.2	7

4 Experimental Setup and Results

The model is invented, studied, and inspected for confirmations. The prototype photographs and the preparation of the resonators are presented in Fig. 5(a), (b). A segment of foam is employed among the dual resonators to attain ideal measurements. The measured results are in good agreement with the simulation as shown in Fig. 5(c).

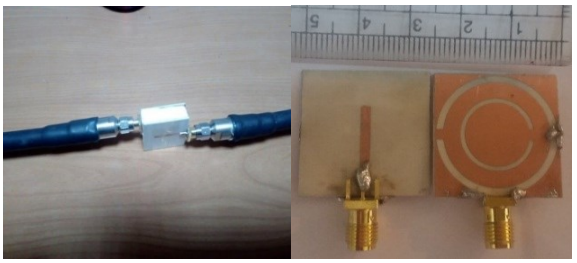

(a)

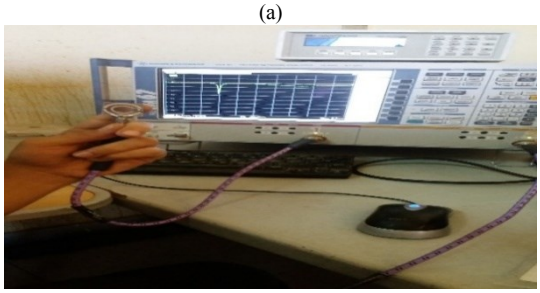

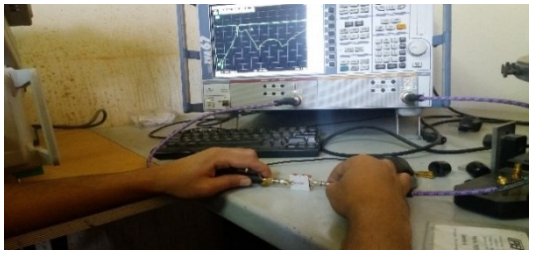

(b)

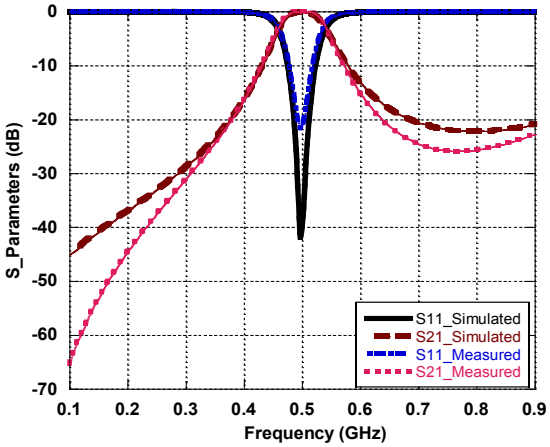

(c)

Fig. 5 (a) Photographs of the fabricated prototype (b) The measurement preparation of the invented design. (c) Comparisons among simulated and measured curves.

5 Coupling Efficiency Calculations

Fig. 6 illustrates the coupling efficiency at 500 MHz, where the simulated $|S_{11}|$ = -42 dB and $|S_{21}|$ = - 0.1 dB. Hence, by employing equation (6) the transmission efficiency equals 97 % at h =16 mm among RX unit and TX unit.

$$\eta_{wpt} = |S_{21}|^2 \sqrt{(1-|S_{11}|^2)(1-|S_{22}|^2)} \quad (6)$$

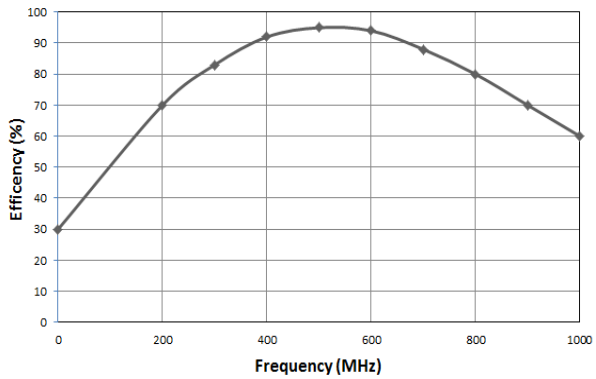

Fig. 6 The coupling efficiency of the resonator

6 Figure-of Merit Assessments

The Figure-of-merit (FoM) of the design can be estimated by equation (7) [20], and Table 3 offers the rapprochements between the suggested manufacture and other earlier researches. Beside the highest coupling efficiency and smallest model size, the suggested single band WPT system possesses the highest FoM that equals 0.62 as shown in Table 3.

$$FoM = \frac{\eta \times h}{\sqrt{L_{sub} \times W_{sub}}} \quad (7)$$

Table 3 The dissimilarities between the suggested model and other earlier works

Design	Size (mm^2)	Operating Frequency (MHz)	h (mm)	Eff. (%)	FoM
This work	25×25	500	16	97	0.62
[26]	20×20	300	13	68	0.442
[22]	25×25	1000	5	85	0.17
[24]	25×25	1000	15	69	0.414
[23]	25×13	3400	12	96	0.6

7 Conclusion

A coupled-resonator model for WPT applications using a shape of CSRRs-DGS loaded with a capacitor is suggested, designed, and verified. The design is analyzed by J-inverter's way and suitable for transferring power with better efficiency of 97 % through a separation distance of 16 mm at 500 MHz resonant band. The measured resonators performance is in good agreement with the simulations.

References

[1] G. W. Wang, Liu M. Sivaprakasam, and G. A. Kendir, "Design and analysis of an adaptive transcutaneous power telemetry for biomedical implants," *IEEE Trans. Circuits Sys. I: Reg. papers*, vol. 52, no. 10, pp. 2109-2117, 2005.

[2] M. Kiani, and M. Ghovanloo, "An RFID-based closed-loop wireless power transmission system for biomedical applications," *IEEE Trans. Circuits Syst. II Express Briefs*, vol. 57, no. 4, pp. 260–264, 2010.

[3] J. Huh, S. W. Lee, W. Y. Lee, G. H. Cho, and C. T. Rim, "Narrow width inductive power transfer system for online electrical vehicles," *IEEE Trans. Power Electron,* vol. 26, no. 12, pp. 3666–3679, 2011.

[4] M. M. A. EL Negm, H. A. Atallah, and A.B. Abdel-Rahman, "Design of dual-band coupled resonators using complementary split ring resonators defected ground structure (CSRRs-DGS) for wireless power transfer applications" 36th National Radio Science Conference (NRSC), Port Said, Egypt, pp. 22-27, 2019.

[5] H. A. Atallah, R. Huseein, and A. B. Abdel-Rahman, "Novel and compact design of capacitively loaded C-shaped DGS resonators for dual band wireless power transfer (DB-WPT) systems" *AEU International Journal of Electronics and Communications,* pp. 95–105, 2019.

[6] Hany A. Atallah "Compact and efficient WPT systems using half-ring resonators (HRRs) for powering electronic devices," *Wireless Power Transfer (WPT)*, vol. 5, no. 2, pp. 105-112, September 2018.

[7] E. K. I. Hamad and H. A. Atallah, "Bandwidth improvement of compact high permittivity RDRA using parasitic conducting strips," *2012 6th European Conference on Antennas and Propagation (EUCAP)*, 2012, pp. 1-4, doi: 10.1109/EuCAP.2012.6206203.

[8] Z. Yalong, H. Xueliang, Z. Jiaming, and T. Linlin, "Design of wireless power supply system for the portable mobile device," *IEEE International Wireless Symposium (IWS)*, pp. 1-4., 2013.

[9] Hany A. Atallah, Adel B. Abdel-Rahman, Kuniaki Yoshitomi, and Ramesh K. Pokharel, "Reconfigurable band-notched slot antenna using short circuited quarter wavelength microstrip resonators," *Progress in Electromagnetic Research C (PIER C)*, vol. 68, pp. 119-127, September 2016.

[10] Hany A. Atallah, Rasha Hussien, and Adel B. Abdel-Rahman, "Compact coupled resonators for small size dual-frequency wireless power transfer (DF-WPT) systems," *IET Microwaves, Antennas & Propagation*, vol. 14, no. 7, pp. 617-628, May 2020.

[11] S. K. Yoon, S. J. Kim, and U.-K. Kwon, "A new circuit structure for near field wireless power transmission," *in IEEE International Symposium on Circuits and Systems (ISCAS),* Seoul, pp. 982–985, 2012.

[12] M. E. Karagozler, J. D. Campbell, G. K. Fedder, S. C. Goldstein, M. P. Weller, and B. W. Yoon. "Electrostatic latching for inter-module adhesion, power transfer, and communication in modular robots," *in IEEE/RSJ International Conference on Intelligent Robots and Systems, San Diego, CA, IROS* , pp. 2779–2786, 2007.

[13] A. Kurs, Karalis, A. R. Moffatt, J. D. Joannopoulos, P. Fisher, and M. Soljoc, "Wireless Power Transfer via Strongly Coupled Magnetic Resonances," *Science,* vol. 317, no. 5834, pp. 83–86, 2007.

[14] H. Matsumoto, "Research on solar power satellites and microwave power transmission in Japan," *IEEE Microw. Mag.*, vol. 3, no. 4, pp. 36–45, 2002.

[15] J. O. Mcspadden, and J. C. Mankins, "Space solar power programs and microwave wireless power transmission technology," *IEEE Microw. Mag.*, vol. 3, no. 4, pp. 46–57, 2002.

[16] R. Hussien, Hany A. Atallah, Sherif Hekal, and Adel B. Abdel-Rahman, "A new design for compact size wireless power transfer applications using spiral defected ground structures," *Radioengineering,* vol. 27, no. 4. , pp. 1032-1037, 2018.

[17] M. Falavarjani, M. Shahabadi, and J. Rashed-Mohassel, "Design and implementation of compact WPT system using printed spiral resonators," *IET Electron. Lett.* vol. 50, no. 2, pp. 110 – 111, 2014.

[18] A. Abdel-Rahman, Verma, A. Boutedjdar, and A. Omar, "A Compact stub type microstrip bandpass filter using defected ground plane," *IEEE Microw. Wirel. Compon. Lett*., vol. 14, no. 4, p. 136–138, 2004.

[19] D. Ahn, et al. "A design of the low-pass filter using the novel microstrip defected ground structure," *IEEE Trans. Microw. Theory Tech*., vol. 49, no. 1, pp. 86–93, 2001.

[20] S. U. Rehman, A. Sheta, and M. Aikanhal, "Compact band stop filter using defected ground structure (DGS)," *Saudi International Electronics, Communications and Photonics Conference (SIECPC)*, *Riyadh*, pp. 1–4, 2011.

[21] M. K. Mandal, and S. Sanyal, "A novel defected ground structure for planar circuits. *IEEE Microw*," *Wireless Compon. Lett.,* vol. 16, no. 2, pp. 93-95, 2006.

[22] S. Hekal, and A. Abdel-Rahman, "New compact design for short-range WPT at 1GHz using H-slot resonators," *9th European Conference on Antennas and Propagation (EuCAP), Lisbon*, pp. 1–5, 2015.

[23] Hany A. Atallah, "Design of compact high efficient WPT system utilizing half ring resonators (HRRs) DGS for short-range applications," *2018 35th National Radio Science Conference (NRSC),* Cairo, Egypt, pp. 63–68, 2018.

[24] R. Sharaf, S. Hekal, and A. B. Abdel-Rahman, "A new compact wireless power transfer system using C-shaped printed resonators," *IEEE Int. Conf. Electron. Circuits Syst. ICECS*, pp. 321–323, 2016.

[25] F. Jolani, Y. Yu, and Z. Cen, "A planar magnetically coupled resonant wireless power transfer system using printed spiral coils," *IEEE Antennas Wireless Propag. Lett*., vol. 65, pp.1648–1651, 2014.

[26] S. Hekal, A. Abdel Rhman, and H. Jia, et al. "A novel technique for compact size wireless power transfer applications using DGS," *IEEE Transactions on Microwave Theory and Techniques*, vol. 65, no. 2, p. 591–599, 2017.

[27] M. H. Mohd Salleh, N. Seman, and D. N. Abangzaidel, et al. "Investigation of unequal planar wireless electricity device for efficient wireless power transfer," *Radioengineering*, vol. 26, no. 1, pp. 251–257, 2017.

[28] M. Palandoken, "Compact bio implantable MICS and ISM band antenna design for wireless biotelemetry applications," *Radioengineering*, vol. 26, no. 4, pp. 917–9232017.

[29] H. J. Visser, "Indoor wireless RF energy transfer for powering wireless sensors," *Radioengineering*, vol. 21, no. 4, p. 963–973, 2014.